NMR T_1-Analysis of Methyl Tunnelling in Molecular Crystals at Intermediate Barriers

H. Langen, A.-S. Montjoie, W. Müller-Warmuth, and Hildegard Stiller
Institut für Physikalische Chemie der Universität Münster

Z. Naturforsch. **42a**, 1266–1274 (1987); received August 20, 1987

The frequency and temperature dependences of the ^{1}H NMR relaxation rates T_1^{-1} for rotating CH_3 groups in solids look quite anomalous at intermediate hindering potential barriers. In order to explain the experimental behaviour and to extract parameters from the NMR T_1 experiments that account for tunnelling at low temperatures and random reorientation at elevated temperatures, we have calculated T_1^{-1} vs. T^{-1} curves to be expected under various conditions. New experimental results for methyl iodide, methyl bromide, 3-methylthiophene, p-xylene, and methyl isocyanate have been fitted by this procedure and all the parameters that describe the motional behaviour have been derived. The single particle rotational potential has been determined using the first two terms of the Fourier expansion.

1. Introduction

Methyl group reorientation in molecular crystals as one of the simplest examples of molecular motion has been extensively studied in recent years by nuclear magnetic resonance (NMR) and inelastic neutron scattering (INS) techniques [1–3]. The purpose of these investigations was to describe the motional mechanism between the limits of the quantum mechanical regime and the thermally activated random rotation, and to determine the magnitude and the shape of the hindering barrier. Because of its simplicity and the continuous transition from tunnelling to classical reorientation the CH_3 rotor provides an ideal model for motional processes in solids in general.

Most direct information can be obtained if the splitting of the torsional ground state is immediately measured by INS. This is possible for potential barriers below about 4.5 kJ/mol corresponding to tunnel splittings larger than 0.5 μeV. For such a situation the NMR frequencies ω_0 usually applied are much smaller than the ground state tunnelling frequencies ω_t^0, and additional data may be derived from NMR to describe the rotation in detail. For higher potential barriers hindering the rotation tunnel splittings can no longer be determined by INS, but the frequency- and temperature dependence of the NMR spin-lattice relaxation rate T_1^{-1} may be used – if possible supplemented by INS studies of torsional transitions – to extract information about the tunnelling mechanism and the barrier. At the usual NMR frequencies drastic anomalies of the T_1^{-1} behaviour are observed below barrier heights of about 7 or 8 kJ/mol. Still more hindered methyl groups may be investigated using double sideband irradiation or other effects upon the NMR lineshape [4].

In the present study we have been interested in the intermediate range of potential barriers where the dependence of T_1^{-1} is characterized in a striking way by tunnelling effects. Many materials possess methyl tunnelling frequencies $\omega_t^0/2\pi$ between 300 and 30 MHz, which correspond to splittings between 1.2 and 0.12 μeV, giving rise to the phenomena discussed in this paper. Typical examples of such a behaviour are already known [5–7], but here we would like to give a more systematic view and to present new experimental results. To illustrate the application of the NMR-T_1 analysis, measurements for methyl iodide, methyl bromide, 3-methylthiophene, p-xylene, and methyl isocyanate will be discussed. In a following paper more results on methyl substituted five-membered heterocyclic rings will be reported.

Reprint requests to Prof. Dr. W. Müller-Warmuth, Institut für Physikalische Chemie der Universität Münster, Schloßplatz 4–7, D-4400 Münster.

0932-0784 / 87 / 1100-1266 $ 01.30/0. – Please order a reprint rather than making your own copy.

2. Presentation of the Frequency- and Temperature Dependence of T_1^{-1}

2.1 Theoretical Background and Approximations

The calculation of the relaxation rate of tunnelling and reorienting methyl groups is essentially based on Haupt's original equation [8, 9]

$$\frac{1}{T_1} = C_{AE} \sum_{-2}^{+2} \frac{n^2 \tau_c}{1 + (\omega_t + n\omega_0)^2 \tau_c^2} + C_{EE} \sum_{1}^{2} \frac{n^2 \tau_c}{1 + n^2 \omega_0^2 \tau_c^2}. \quad (1)$$

The first term accounts for dipole-dipole interactions within a methyl group ("intramethyl"), the second term for those of the protons of one methyl group with other protons ("intermethyl"). The relaxation constants C_{AE} and C_{EE} may be written [6, 9, 10]

$$C_{AE} = \frac{9}{40}\delta^2 \left(\frac{\mu_0}{4\pi}\right)^2 \frac{\gamma^4 h^2}{b^6} p(1 + X_1),$$
$$C_{EE} = \frac{9}{20}\delta^2 \left(\frac{\mu_0}{4\pi}\right)^2 \frac{\gamma^4 \hbar^2}{b^6} p X_2, \quad (2)$$

where μ_0, γ and $\hbar$ have the usual meaning. The relaxation efficiency factor δ^2 is of the order of magnitude of 1. $b = 178.1$ pm is the proton-proton distance in the CH_3 group, and p denotes the ratio of methyl protons to the total number of protons. X_1 and X_2 account for the intermethyl contribution in a phenomenological way. The temperature dependence of the correlation time τ_c is approximated by

$$\tau_c^{-1} = (\tau_0')^{-1} \exp(-E_A'/RT) + (\tau_0'')^{-1} \exp(-E_A''/RT). \quad (3)$$

The limiting value E_A' may be identified with the activation energy E_A. E_A'' approaches E_{01}, the energy separation between the torsional ground and first excited states, only if the potential barrier is low.

Application of (1) and (3) for evaluating experimental data has to consider furthermore the temperature dependence of the tunnelling frequency ω_t and the non-exponential character of the relaxation. Examination of various experimental data suggests that

$$\omega_t(T) = \omega_t^0/(1 + a T^6) \quad (4)$$

is a reasonable approximation to describe the temperature dependence of ω_t. The coefficient a is characteristic of the respective system. The non-exponentiality of the relaxation is a consequence of the symmetry-restricted spin diffusion [10–12]. T_1^{-1} of (1) has to be identified with the initial slope of the plot of $\ln\{(M_0 + M_z)/M_0\}$ against time measured after the spin system has been properly prepared (M_0 equilibrium magnetization, $M_z(t)$ component of the partially relaxed spin system in field direction).

2.2 Graphic Representation

In this paragraph we present a great variety of anomalous T_1^{-1} versus $1/T$ curves that may be calculated and compared with the experiment. To obtain a general survey of the dependence on various parameters we computed T_1^{-1} using (1), (3) and (4) for two NMR frequencies which differ by a factor of 2. Figure 1 shows the results for decreasing tunnelling frequencies (from top to bottom). On the right hand side ω_t^0 is more strongly dependent on temperature than on the left. The relation between ω_t^0 and E_A, and the numerical values for τ_0', τ_0'', E_A'', C_{AE} and C_{EE} correspond as well as possible to those of the known experimental data. We have also calculated the curves for $\omega_t/2\pi = 10$ MHz (not shown) which, however, can no longer be distinguished from a classical BPP [13] behaviour.

Figure 2 accentuates the importance of the relative contributions of intra- and inter-methyl interactions in (1). Different C_{AE}/C_{EE} ratios change the curves in particular for large tunnelling frequencies, if separate frequency-dependent and frequency-independent relaxation maxima are observed.

The influence of τ_0'' in (3) is shown in Figure 3. Whereas the experimental limiting high temperature correlation time τ_0' is always of the same order of magnitude, τ_0'' varies greatly as a function of the potential barrier. This is a consequence of the approximation (3), in which τ_0'' is only well defined at low barriers, where E_A'' approaches E_{01}. Comparison of the various curves of Fig. 3 demonstrates that the accuracy of a determination of the parameters E_A'' and τ_0'' from the slope and the maxima is rather poor since the limiting low temperature behaviour is not accessible at intermediate barriers.

2.3 Examples of Previous Results

Most of the relaxation dependences that were determined previously and interpreted in terms of CH_3 tunnelling correspond to the limiting case of Fig. 1 a

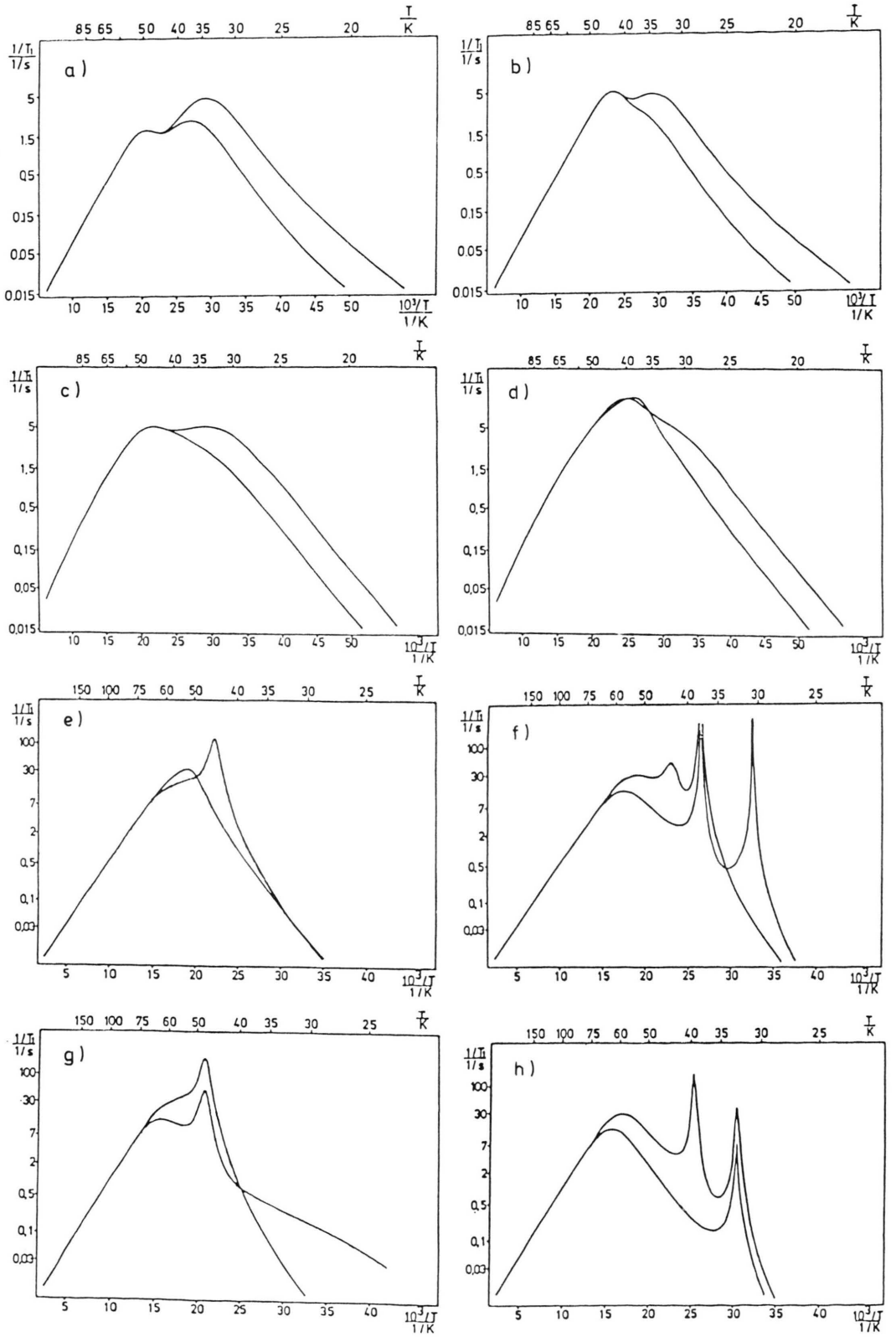
a)
b)
c)
d)
e)
f)
g)
h)
T/K
1/T1/1/s
10³/T 1/K

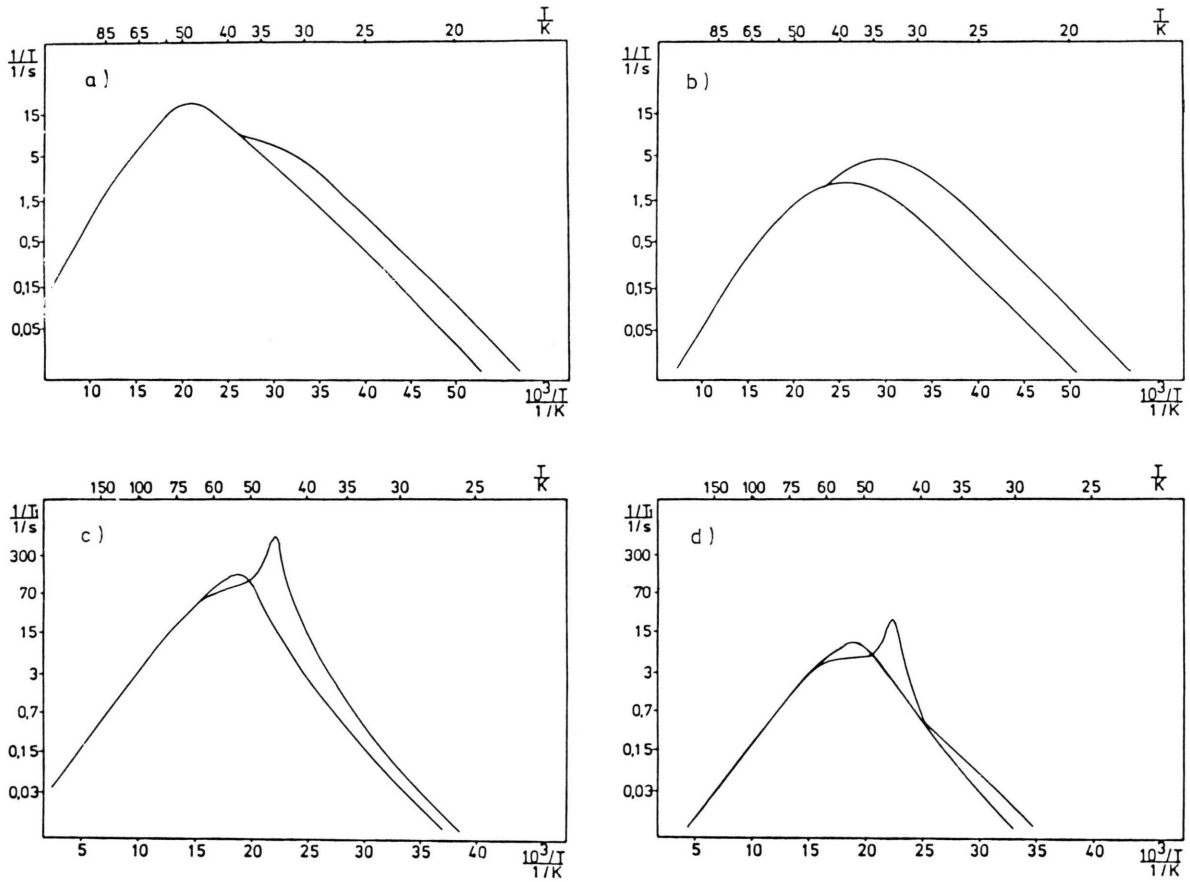

Fig. 2. Dependence of the computed relaxation curves on $C_{AE}/C_{EE} = 13.3$ (a, c), 0.53 (b, d) for $\omega_t^0/2\pi = 300$ MHz (a, b) and 100 MHz (c, d). These curves may be compared with those of Fig. 1 (a, c, e, g), where $C_{AE}/C_{EE} = 2.67$ is kept constant and otherwise the same parameters were used.

and b, e.g. toluene [14, 15], 3-methylpyridine [9], and sodium acetate [1]. Sometimes the experimental curves look similar but can only be described assuming nonequivalent methyl groups [16, 17]. Experimental examples for other curve shapes, such as those shown in Fig. 1 c–h, are 3,5-dimethylpyridine, [9] tetramethylsilane and tetramethylgermanium [5]. Further studies will be discussed in the next chapters and in a following paper. In contrast to previous investigations we apply now the procedure developed in this chapter to fit the experimental curves using the complete formula (1) and a temperature-dependent tunnelling frequency, (4).

3. Experimental Details and Results

The materials listed in Table 1 were purchased from Fluka, Aldrich or Riedel-de Häen companies and were further purified by distillation if necessary. They were carefully dried using molecular sieves, and oxygen was removed by several freeze-pump-thaw cycles. The samples were than sealed in glass ampoules.

Fig. 1. Dependence of the computed relaxation curves on the tunnel frequency and its temperature dependence for $\omega_0/2\pi = 30$ and 15 MHz: $\omega_t^0/2\pi = 1000$ MHz, $E_A = 3.0$ kJ/mol (a, b); 300 MHz, 4.1 kJ/mol (c, d); 100 MHz, 4.9 kJ/mol (e, f); 60 MHz, 5.4 kJ/mol (g, h). Curves a, c, e, g on the left hand side belong to a coefficient $a = 8 \cdot 10^{-11}\,K^{-6}$; curves b, d, f, h on the right hand side to $a = 8 \cdot 10^{-10}\,K^{-6}$. The further prameters are $E_A'' = 1.3$ kJ/mol (a, b), 2.0 (c, d), 3.5 (e, f), 4.0 (g, h); $\tau_0' = 2 \cdot 10^{-13}$ s; $\tau_0'' = 5 \cdot 10^{-10}$ s (a, b) and $5 \cdot 10^{-12}$ s (c–h); $C_{AE} = 10 \cdot 10^8\,s^{-2}$; $C_{EE} = 3.75 \cdot 10^8\,s^{-2}$.

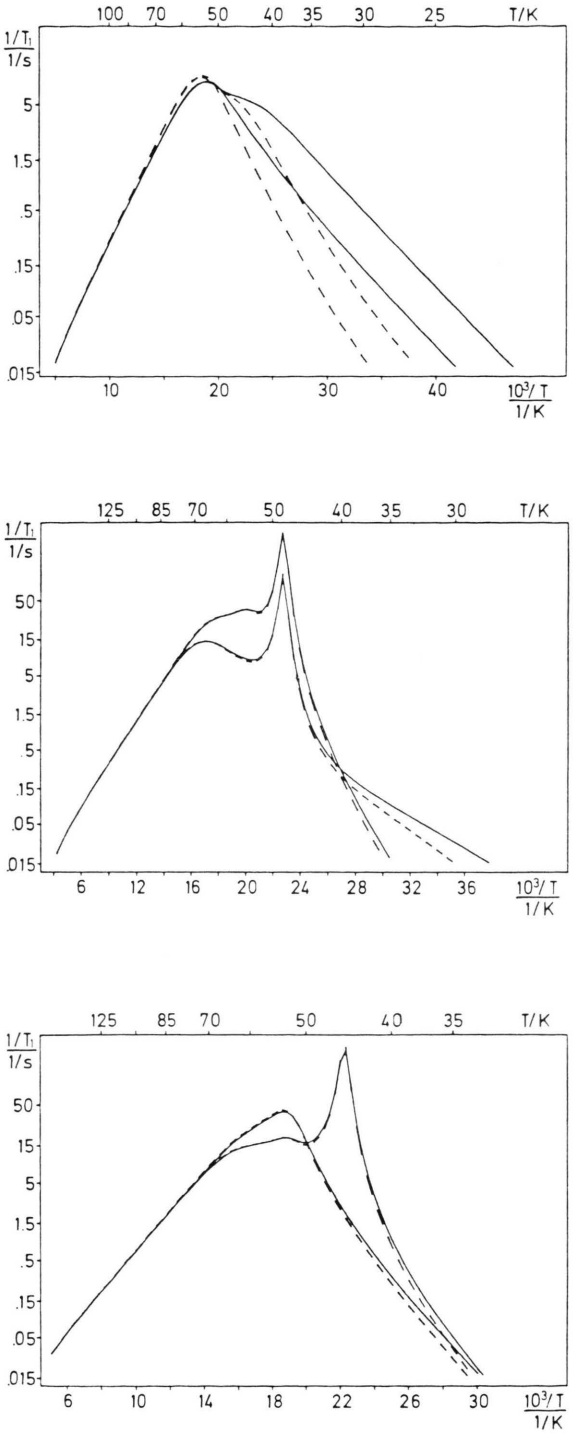

Fig. 3. Computed T_1^{-1} vs. T_{-1} curves for different τ_0'' parameters ($5 \cdot 10^{-11}$ s: solid line, $5 \cdot 10^{-10}$ s: dotted line) and tunnel frequencies of 300 MHz (a), 100 MHz (b), 60 MHz (c) and 10 MHz (d). The other parameters are the same as in Fig. 1 c, e, g.

NMR experiments were carried out using a Bruker SXP pulsed spectrometer at frequencies of $\omega_0/2\pi = 15$ and 30 MHz. $90° - \tau - 90°$ pulse sequences were applied and $1/T_1$ was determined from the initial slope of the plot $\ln\{(M_0 - M_z)/M_0\}$ against time as already explained. The accuracy of the $1/T_1$ determination suffers from the non-exponentiality and is only of the order of $\pm$ 10% and even less in unfavourable cases. Continuous flow liquid helium cryostats from Oxford Instruments with PID control units were employed, and the temperature was independently measured near the sample by Ni-Cr/Au-0.02 at% Fe-thermocouples. The accuracy of the temperature measurement is $\pm$ 0.5 K.

Level-crossing spectroscopy [18, 19] was applied to measure the tunnelling frequencies directly by NMR in those cases where a determination by INS is no longer possible. We used a home-made and fully automated field cycling spectrometer to record the relaxation peaks that occur when the Zeeman and tunnel splittings match. Figure 4 shows such "tunnel peaks" for 3-methylthiophene and methylisocyanate. The ω_t^0 values in Table 1 were immediately derived from these experiments.

For the methyl halides both ω_t^0 and E_{01} were already measured by INS [20]. The torsional transitions E_{01} for 3-methylthiophene and p-xylene were also

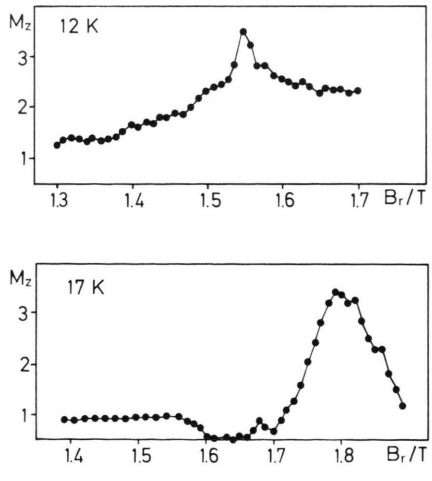

Fig. 4. Field cycling spectra for 3-methylthiophene (top) and methyl isocyanate (bottom). The M_z component of the magnetization in arbitrary units is plotted against the magnetic reference field B_r which is varied in steps of 0.01 T.

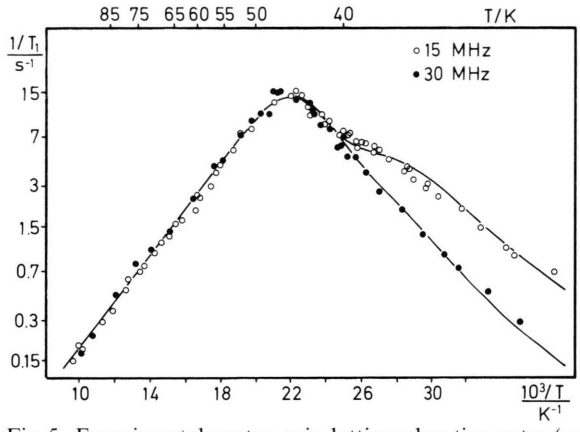

Fig. 5. Experimental proton spin-lattice relaxation rates (as defined in the text) for methyl iodide vs. reciprocal temperature (points). The solid lines correspond to the best fit using the procedure outlined in this paper. The parameters of the fit are given in Table 1.

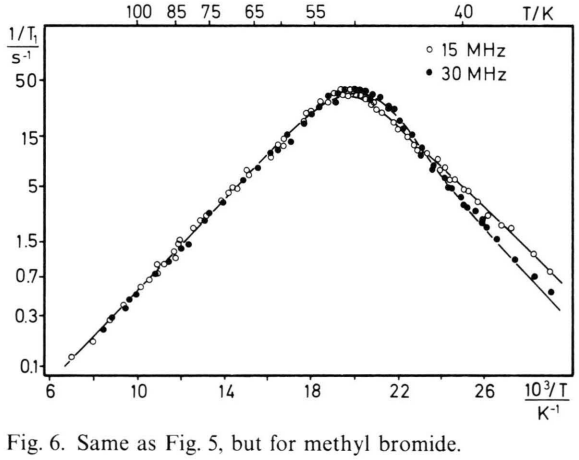

Fig. 6. Same as Fig. 5, but for methyl bromide.

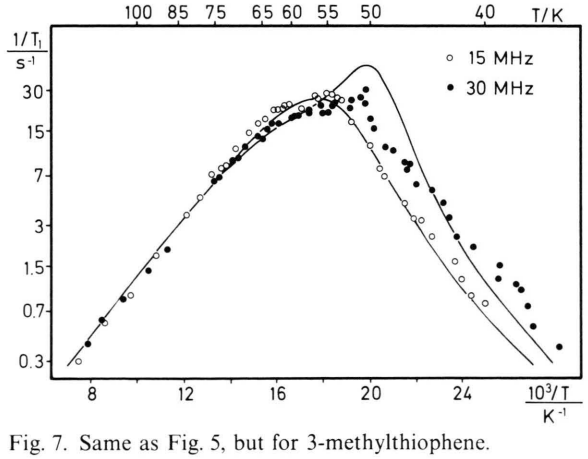

Fig. 7. Same as Fig. 5, but for 3-methylthiophene.

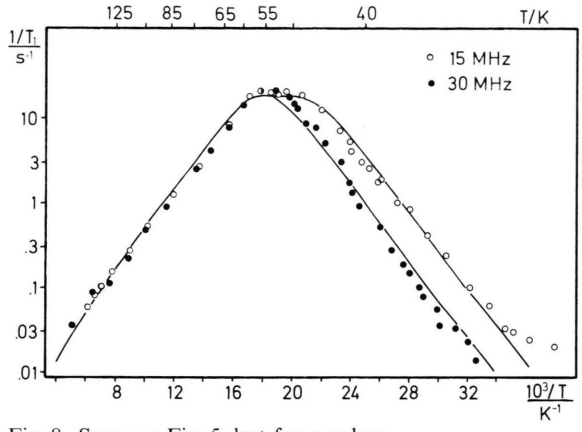

Fig. 8. Same as Fig. 5, but for p-xylene.

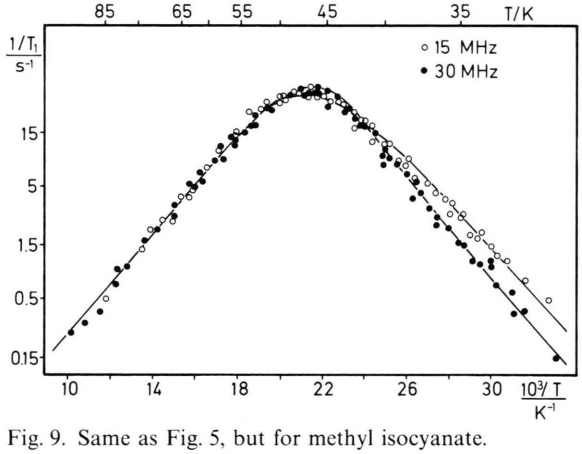

Fig. 9. Same as Fig. 5, but for methyl isocyanate.

measured in Jülich using the thermal time of flight spectrometer SV 22 [21].

The results of the $1/T_1$-measurements and curve fittings are shown in Figures 5–9. The relaxation rates of methyl iodide (Fig. 5) are distinguished by an important frequency-independent maximum characteristic of the conditon $\omega_t \tau_c = 1$; they can be fitted by curves which lie between those of Figs. 1 b and 2 a. The relaxation of methyl bromide (Fig. 6) possesses very little frequency dependence at all; a theoretical description is similar to Fig. 2 c with a level-crossing maximum $\omega_t = 2\omega_0$ which, however, is no longer visible since it is shifted a little bit more to the left hand side. The experimental data of 3-methylthiophene (Fig. 7) and methyl isocyanate (Fig. 9) are reminiscent of Figure 1 e. In the first case the level crossing maximum $\omega_t = 2\omega_0$ is visible, in the second not. p-xylene

(Fig. 8) finally is interpreted in terms of parameters which are not too far from those of Figure 1 c.

The solid lines of Figs. 5–9 were obtained by the same computer programs which were used for the graphic representation of (1). The tunnelling frequencies of the torsional ground state – if available – were taken as given, the other parameters of Table 1 correspond to the best fits of the experimental points.

4. Discussion

The present study shows in addition to previous work that on the whole the experimental relaxation rates may be described by (1) and the approximations applied in Chapter 2. The curve fits thus obtained reproduce the measurements quite well and result in parameters which are important for the description of the motional process. In contrast to the theoretical relaxation rates, however, in the experiment the level crossing peaks occurring at $\omega_t = \omega_0$ and $\omega_t = 2\omega_0$ appear to be much less pronounced. Nevertheless, apart from this fact the anomalous relaxation curve shapes to be expected from the theory are really observed.

Inspection of Table 1 confirms the correlation between the activation energy E_A and the ground state tunnel splitting ω_t^0 which was already stated previously for other methyl rotors [1, 5]. The extraordinary temperature dependence of the tunnelling frequency for methyl iodide obtained from the fit is in accordance with INS data [20]. The torsional splitting E_{01} in the fourth column has been determined independently from NMR by inelastic neutron scattering techniques [20, 21]; only at low hindering potentials (CH_3I) it agrees with the apparent low temperature activation energy E_A''. The high temperature prefactor τ_0' is always of the same order of magnitude. Together with the value of E_A it describes the classical reorientation of the CH_3-groups.

τ_0'' and E_A'' are only well defined for cases where the low temperature relaxation is governed by tunnel transitions combined with non-magnetic excitations from the torsional ground state. E_A'' then approaches E_{01}, and τ_0'' is in between 10^{-10} and 10^{-9} s [8]. Such a situation is generally realized for potential barriers lower than about 3.5 kJ/mol; further examples are toluene [15], m-xylene [22, 23], 3-methylpyridine [9], sodium acetate [1], and 2-methylthiophene [24]. At intermediate barriers as met for most of the compounds of this study, more torsional transitions come into play, and both E_A'' and τ_0'' are neither well defined nor accurately determined. The order of magnitude of the relaxation constants C_{AE} and C_{EE} corresponds to $C_{AE}/[\delta^2 \cdot p(1 + X_1)] = 40 \cdot 10^8\,s^{-2}$, (2). No systematic dependences upon the various parameters were found. This behaviour agrees with what we know from previous studies.

4.1 Rotational Potential

The data may be used to determine the hindering potential quite accurately. The rotational potential $V(\varphi)$ is generally described by a Fourier expansion with the basic threefold symmetry of the CH_3-group, where the development is restricted to the first two terms:

$$V(\varphi) = \frac{V_3}{2}[1 + (-1)^k \cos 3\varphi] + \frac{V_6}{2}[1 + (-1)^k \cos 6\varphi]. \quad (5)$$

The eigenvalues of the Schrödinger equation with this potential are tabulated [25]. Using the experimental

Table 1. Numerical parameters for the various materials as derived from the measurements and the fitting procedures. Asterisks refer to INS studies, references * [20] and ** [21]. A bracket means no direct measurements of the tunnel splitting as in all other cases.

Molecular crystal	E_A kJ/mol	$\omega_t^0/2\pi$ MHz	E_{01} kJ/mol	E_A'' kJ/mol	τ_0' 10^{-13} s	τ_0'' 10^{-11} s	C_{AE} $10^8\,s^{-2}$	C_{EE} $10^8\,s^{-2}$	a $10^{-11}\,K^{-6}$
methyl iodide	3.3	590*	1.28*	1.2	1.4	80	31	3.3	34
methyl bromide	4.1	218*	1.52*	3.0	0.95	2	50	3.7	7.4
3-methylthiophene	4.5	129	1.72**	2.8	5.3	2	16	0.5	6.2
p-xylene	4.5	(334)	1.54**	3.4	1.0	2	21	13	6.0
methyl isocyanate	4.6	151	–	3.7	0.40	0.03	39	8.1	6.0

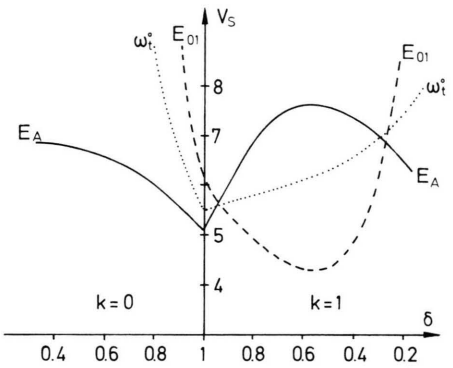

Fig. 10. Graphic determination of $V_s(\delta)$ using the experimental values of the activation energy E_A, the tunnel splitting $\hbar\omega_t^0$, and the torsional excitation E_{01} in combination with the solutions of the Schrödinger equation for 3-methylthiophene as an example.

Table 2. Single particle rotational potentials as derived from the experimental data.

Molecular crystal	Solution I			Solution II		
	k	$\frac{V_s}{\text{kJ/mol}}$	δ	k	$\frac{V_s}{\text{kJ/mol}}$	δ
methyl iodide	0	4.2	0.96	1	5.4	0.27
methyl bromide	0	4.9	0.99	1	6.5	0.27
3-methylthiophene	1	5.6	0.94	1	6.9	0.28
p-xylene	0	5.3	0.98	1	6.9	0.24
methyl isocyanate		5.4	1	1	7.0	0.23

values for the activation energy E_A (energy separation between the barrier and the torsional ground state) and the tunnel splitting $\hbar\omega_t^0$, the two parameters V_3 and V_6 can be obtained from the tabulated solutions. If we know in addition the torsional frequency E_{01}, the system is overdetermined. This means, among the parameters E_A, $\hbar\omega_t^0$, E_{01} at least two have to be known in order to derive the third one and the potential. If all three are available there is additional control that the data belong to the same solution. This is demonstrated graphically in Figure 10. The rotational potential is characterized by $V_s = V_3 + V_6$ and $\delta = V_3/V_s$; E_A, $\hbar\omega_t^0$, and E_{01} are drawn for all values of V_s and δ which are possible from the solution tables. The intersection gives then two solutions, one for a phase factor $k = 0$ and the other one for $k = 1$.

Corresponding solutions were obtained for all five materials, Table 2. Neutron scattering studies of isotope effects revealed for methyl iodide and methyl bromide that the second solution with a dominant sixfold potential can be rejected [20]. Also in agreement with a general systematics [1], solution I is most probably the correct solution in each case. This potential is not far from a threefold cosine potential but the minima tend to be slightly broadened.

4.2 Individual Results

Inspection of the results of Tables 1 and 2 shows the rotational behaviour of methyl rotors at intermediate barriers for increasing activation energies. Depending on the precise shape of the hindering potential of the various materials the total barrier V_s and the tunnel frequency ω_t^0 do not necessarily change in the same order. Considering the results in detail, for CH_3I and CH_3Br a part of the information was already available from INS studies [20]; the parameters extracted from the T_1-measurements are in agreement with the conclusions of Prager et al. The dipolar interaction within a CH_3 group is much stronger than that between different groups, which leads to a rather large C_{AE}/C_{EE} ratio. INS, NMR, and a known crystal structure [26] provide a rather complete description of the molecular dynamics. For 3-methylthiophene both rotational tunnelling and classical reorientation has been completely explored by NMR; the results will be discussed in connection with other five-membered ring systems in a following paper. p-xylene belonged to the first materials which revealed rotational tunnelling at all [22], but at that time the symmetry-restricted spin diffusion was not considered, and we did not understand the anomalous frequency dependence. The data are characteristic of a relatively large tunnel splitting and an important influence of the intermethyl dipolar interaction. Methyl isocyanate finally is distinguished by a purely threefold potential barrier; all parameters are derived from NMR.

Acknowledgement

The financial support of this research by the Deutsche Forschungsgemeinschaft is gratefully acknowledged.

[1] A. S. Montjoie and W. Müller-Warmuth, Z. Naturforsch. **40 a,** 596 (1985), and references therein.
[2] W. Press, Single-Particle Rotation in Molecular Crystals, Springer Tracts in Modern Physics, Springer-Verlag, Berlin 1981.
[3] Review: D. Cavagnat, J. Chim. Phys. **82,** 239 (1985), and references therein.
[4] P. J. McDonald, G. J. Barker, S. Clough, R. M. Green, and A. J. Horsewill, Mol. Phys. **57,** 901 (1986), and references therein.
[5] W. Müller-Warmuth, K. H. Duprée, and M. Prager, Z. Naturforsch. **37 a,** 66 (1984).
[6] D. J. Ligthelm, R. A. Wind, and J. Smidt, Physica **100 B,** 175 (1980).
[7] W. T. Sobol, K. R. Sridharan, I. G. Cameron, and M. M. Pintar, Z. Naturforsch. **40 a,** 1075 (1985).
[8] J. Haupt, Z. Naturforsch. **26 a,** 1578 (1971).
[9] W. Müller-Warmuth, R. Schüler, M. Prager, and A. Kollmar, J. Chem. Phys. **69,** 2382 (1978).
[10] B. Gabrys and L. Van Gerven, J. Phys. C: Solid State Phys. **18,** 1241 (1985).
[11] S. Emid and R. A. Wind, Chem. Phys. Lett. **33,** 269 (1975).
[12] S. Emid, R. J. Baarda, J. Smidt, and R. A. Wind, Physica **93 B,** 327 (1978).
[13] N. Bloembergen, E. M. Purcell, and R. V. Pound, Phys. Rev. **73,** 679 (1984).
[14] J. Haupt and W. Müller-Warmuth, Z. Naturforsch. **24 a,** 1066 (1969).
[15] W. Müller-Warmuth, R. Schüler, M. Prager, and A. Kollmar, J. Magn. Resonance **34,** 83 (1979).
[16] M. Prager, K. H. Duprée, and W. Müller-Warmuth, Z. Phys. B-Condensed Matter **51,** 309 (1983).
[17] M. Prager and W. Müller-Warmuth, Z. Naturforsch. **39 a,** 1187 (1984).
[18] P. Van Hecke and J. Janssens, Phys. Rev. B **17,** 2124 (1978).
[19] B. Gabrys, Mol. Phys. **51,** 601 (1984), and references therein.
[20] M. Prager, J. Stanislawski, and W. Häusler, J. Chem. Phys. **86,** 2563 (1987).
[21] We are grateful to Dipl.-Chem. J. Stanislawski for carrying out these measurements.
[22] J. Haupt and W. Müller-Warmuth, Z. Naturforsch. **23 a,** 208 (1968).
[23] M. Prager, private communication.
[24] To be published.
[25] R. F. Gloden, Euratom Reports EUR 4349 and EUR 4358 (1970) and supplements by M. Prager, Jülich.
[26] L. W. G. Wyckoff, Crystal Structures, Vol. 1, John Wiley, New York 1964.